ISTANBUL TECHNICAL UNIVERSITY ★ GRADUATE SCHOOL OF SCIENCE

GRADUATE SCHOOL OF SCIENCE

AUTOMATED SCORING OF CERBB2 RECEPTORS USING HISTOGRAM BASED ANALYSIS OF IMMUNOHISTOCHEMISTRY BREAST CANCER TISSUE IMAGES

M.Sc. THESIS

Kaan Aykut KABAKÇI

Informatics Institute

Applied Informatics Programme

JUNE 2019

ISTANBUL TECHNICAL UNIVERSITY ★ GRADUATE SCHOOL OF SCIENCE

GRADUATE SCHOOL OF SCIENCE

AUTOMATED SCORING OF CERBB2 RECEPTORS USING HISTOGRAM BASED ANALYSIS OF IMMUNOHISTOCHEMISTRY BREAST CANCER TISSUE IMAGES

M.Sc. THESIS

Kaan Aykut KABAKÇI
(708161010)

Informatics Institute

Applied Informatics Programme

Thesis Advisor: Assoc. Prof. Dr. Behçet Uğur TÖREYİN

JUNE 2019

İSTANBUL TEKNİK ÜNİVERSİTESİ ★ FEN BİLİMLERİ ENSTİTÜSÜ

İMMÜNOHİSTOKİMYA MEME KANSERİ GÖRÜNTÜLERİNİN HİSTOGRAM TABANLI ANALİZ KULLANILARAK CERBB2 RESEPTÖRLERİNİN OTOMATİK OLARAK SKORLANMASI

YÜKSEK LİSANS TEZİ

Kaan Aykut KABAKÇI
(708161010)

Bilişim Enstitüsü

Bilişim Uygulamaları Ana Bilim Dalı

Tez Danışmanı: Assoc. Prof. Dr. Behçet Uğur TÖREYİN

HAZİRAN 2019

Kaan Aykut KABAKÇI, a M.Sc. student of ITU Graduate School of Science Engineering and Technology 708161010 successfully defended the thesis entitled "AUTOMATED SCORING OF CERBB2 RECEPTORS USING HISTOGRAM BASED ANALYSIS OF IMMUNOHISTOCHEMISTRY BREAST CANCER TISSUE IMAGES", which he/she prepared after fulfilling the requirements specified in the associated legislations, before the jury whose signatures are below.

Thesis Advisor :	**Assoc. Prof. Dr. Behçet Uğur TÖREYİN** Istanbul Technical University	.....
Jury Members :	**Dr. Nazim Kemal URE** Istanbul Technical University	.....
	Dr. Murat GEZER Istanbul University	.....
		.....

Date of Submission : **3 May 2019**
Date of Defense : **13 July 2019**

To my wife,

FOREWORD

First of all, I would like to thank my thesis supervisor Assoc. Prof. Dr. Behçet Uğur TÖREYİN, who has great efforts in the preparation of my master thesis and who has never retired from their support. I would also like to thank Dr. Abdulkerim ÇAPAR, who is always on my side, providing continuous access to the data set required for the thesis, with continuous support in the processing of the data.In addition, I would like to thank the faculty members of Medipol University Pathology Department which provides the first set of pathological data used in the thesis phase and the Argenit Company family, which allows digitization of these data through a microscope. I also would like to thank Warwick University Computer Science Department doctoral student Talha QAISER and Prof. Dr. Nasir RAJPOOT for providing us with remote access to the pathological data they have.

June 2019 Kaan Aykut KABAKÇI

TABLE OF CONTENTS

Page

ABBREVIATIONS

IHC	**:** Immuno Histo Chemistry
H	**:** Hematoxylin
DAB	**:** Diaminobenzidine
CT	**:** Chemotherapy
EGFR	**:** Epidermal Growth Factor Receptor
ISH	**:** In Situ Hybridization
FISH	**:** Fluorescent in Situ Hybridization
MIH)	**:** Membrane Intensity Histogram
MCD	**:** Minimum Cluster Distance
HSV	**:** Hue, Saturation, Value
SVM	**:** Support Vector Machine
MLP	**:** Multilayer Perceptron
KNN	**:** K Nearest Neighbors
LSTM	**:** Long Short-Term Memory
CCD	**:** Charge Coupled Device
WSI	**:** Whole Slide Image
T	**:** Transformation Matrix

SYMBOLS

D	**:** DAB Channel
H	**:** Hematoxylin Channel
HB	**:** Binary Image of Hematoxylin Channel
HD	**:** Distance Transform of HB
P_{cc}	**:** Cell Center Point
PPList	**:** Cell Membrane Polygon Point List
R_{D_B}	**:** Binary Image of Diaminobenzidine Channel of Tissue Region
C_{Av_θ}	**:** Average intensity value of the pixels along the $\theta - th$ direction
$C_Q^{'}$	**:** q^{th} MIH Value of the Cell Under Consideration
R_i	**:** i^{th} Region of tissues.
R_{i_H}	**:** Hematoxylin Channel of the i^{th} Region of Tissue.
C_i	**:** i^{th} Cell of the i^{th} Region of Tissue.
R_{i_D}	**:** DAB Channel of the i^{th} Region of Tissue.
C_{i_H}	**:** Hematoxylin Channel of the i^{th} Cell.
C_{i_D}	**:** DAB Channel of the i^{th} Cell.
$C_{i_{H_B}}$	**:**Binary Image of Hematoxylin Channel of the i^{th} Cell.
$C_{i_{D_B}}$	**:**Binary Image of DAB Channel of the i^{th} Cell.
H_i	**:** Histogram of the i^{th} Cell.
$R_iC_jV_n$	**:** n^{th} vector member of MIH vector of j^{th} cell of i^{th} Region of the tissue.

LIST OF TABLES

Page

LIST OF FIGURES

Page

AUTOMATED SCORING OF CERBB2 RECEPTORS USING HISTOGRAM BASED ANALYSIS OF IMMUNOHISTOCHEMISTRY BREAST CANCER TISSUE IMAGES

SUMMARY

In this study, novel image analysis techniques for scoring CerbB2 receptors in breast cancer tissue specimen images of patients with suspected breast cancer are proposed. Visual expression of invasive breast cancer with immunohistochemistry(IHC) allows evaluation of CerbB2 receptors. In invasive breast cancer, tumors are evaluated in 4 different stages as Score 0, Score 1, Score 2 and Score 3 by applying IHC method. Score 3 tumors are considered suitable for treatment specific to the CerbB2 protein, which is considered ineffective for score 0 and score 1. Score 2 is the borderline which means some tumors can benefit from treatment. Throughout this analysis, new modalities in the treatment which is called 'targeted therapy' is used for pathological assessment of the receptor status in the tumor with CerbB2 receptors, therefore a therapy is advised for breast cancer. For this purpose, pathological images obtained by using Immunohistochemistry (IHC) were analyzed to determine CerbB2 score levels at cellular level. Two different datasets were obtained for use in the study. The first dataset was digitized by using microscope and camera from the obtained tissue slides. The second dataset is obtained from a dataset that can be accessed publicly. Firstly, images are separated into hematoxylin (H-Blue) and diaminobenzidine (DAB-Brown) color channels and cell centers and cell membranes are determined. Subsequently, membrane intensity histograms are extracted by the proposed image analysis method, so features for each cell are obtained. Finally, obtained attributes are trained with some classifiers like Long-Short Term Memory(LSTM), KNN, Decision Trees, obtained by experimental methods, therefore classification models was created. The datasets were classified as both cell-based and image-based. The CerbB2 scoring system consisting of 4 classes image-based classification has left behind similar methods with 91,43% accuracy. As for the accuracy of cell-based accuracy, 77,56% was achieved and it was predicted that this accuracy could be increased in future studies. Each step in the study is explained in detail and experimental results are presented in comparison to other state-of-the-art methods.

İMMÜNOHİSTOKİMYA MEME KANSERİ GÖRÜNTÜLERİNİN HİSTOGRAM TABANLI ANALİZ KULLANILARAK CERBB2 RESEPTÖRLERİNİN OTOMATİK OLARAK SKORLANMASI

ÖZET

Bu çalışmada, meme dokusunda şüpheli durumla karşılaşılan hastaların meme dokusu görüntülerinde mutasyona uğramış CerbB2 reseptörlerini puanlamak için yeni görüntü analiz tekniği önerilmiştir. Invaziv meme kanserinin immünohistokimya(ImmunoHistoChemistry) ile boyanarak tümör hücrelerinin çeperinde oluşan boyanma miktarından ve boyanmanın hücreyi çevrelemesinden yola çıkılarak CerbB2 reseptörlerinin değerlendirilmesi sağlanır. İnvaziv meme kanserinde tümörler, IHC yöntemiyle 0+, 1+, 2+ ve 3+ olmak üzere 4 farklı aşamada değerlendirilir. Skor 3+ olarak tanımlanmış tümörler CerbB2 proteinine özgü bir tedaviye uygun olarak kabul edilir. Skor 0+ ve Skor 1+ için bu tedavi etkisiz kabul edilir. Skor 2, bazı tümörlerin tedavinin işe yarayacağı veya tedavi alması gerektiği anlamına gelen sınır çizgisidir. Kısaca açıklayacak olursak bu skorlama yöntemi kanser hastasının hangi tedaviyi alması gerektiğini belirler. Görsel anlamda da ifade edersek, Skor 3+ tipinde sınıflandırılan dokularda tamamıyla hücre çeperi boyanmış ve boyamanın yoğun olduğu hücre sayısı bütün tümör bölgesinde bulunan hücre saysının %10'undan fazladır. Çevresel hücre çeperi boyanması tamamlanmamış ve orta derece yoğunlukta boyama olan hücrelerin sayısı %10'dan fazla veya çevresel hücre çeperi boyanması tamamlanmış ve yoğun boyanmış hücre sayısı %10'dan küçük ve %1'den daha fazla bulunuyorsa bu özellikleri gösteren dokular Skor 2+ olarak değerlendirilmektedir. Skor 3+ pozitif olarak değerlendirilirken Skor 2+ belirsiz olarak değerlendirilmekte ve bu tür vakalar altın standart(gold standard) olarak tanımlanan Florosan In Situ Hibritleme(Fluorescence In Situ Hybridization-FISH) yöntemi ile genetik olarak incelenerek tanımlanmaktadır. FISH sonucu eğer pozitif çıkarsa Skor 3+ gibi bir tedavi, negatif çıkarsa Skor 1+ gibi bir tedavi uygulanır. Çevresel boyonması zayıf ve zar zor seçilebilen ve tamamen çevrelemeyen hücre sayısı %10'un üzerinde olan ve ilk iki şartı sağlamayan tümörler Skor 1+ olarak değerlendirilmektedir. Bu üç şartı sağlamayan tümörler ise Skor 0+ olarak değerlendirilir ve Skor 1+ ile Skor 0+ özelliği gösteren tümörler negatif olarak değerlendirilmektedir.

Bu analizler çerçevesinde, yeni bir tedavi yöntemi olarak önerilen 'hedefli tedavi', CerbB2 reseptörleri ile tümördeki reseptör durumunun patolojik olarak değerlendirilmesinde kullanılır ve kişiye özel bir kanser tedavisi önerilir. Buradaki en önemli handikap ise Skor 2+ olarak tanımlanan vakalarda yaşanan belirsizliklerdir. Bazı vakalarda patologlar tek başlarına karar vermekte zorlanıp ek görüş almak isterler. Aynı vaka için iki farklı patolog iki farklı skor verebilmektedir ve bu da gözlemciler arası tutarsızlığa(Interobserver Discrepancy) sebep olmaktadır. Bu tezde hedeflenen ise patologlara bir ek görüş olacak başarımlar veren bir sınıflandırma aracı geliştirip, bunun tanı koyma aşamasına katkı vermesini sağlamaktır. Bu amaçla, immünohistokimya (IHC) kullanılarak boyanmış farklı iki kanaldan elde edilen patolojik görüntüler, hücre ve tümör bölgesi düzeylerinde CerbB2 skor seviyelerini belirlemek için analiz edilmiştir.

Çalışmada kullanılmak üzere iki farklı veri seti elde edilmiştir. İlk veri seti, Medipol Üniversitesi Patoloji Ana Bilim Dalı'ndan elde edilen doku slaytları kullanılarak mikroskop ve kamera aracılığı ile 40X büyütmede dijitalleştirilmiştir. Bu veri kümesinde 13 farklı doku örneğinden 198 adet görüntü bulunmaktadır. Bu 191 görüntünün 41 tanesi 'Skor 0+', 42 tanesi 'Skor 1+', 52 tanesi 'Skor 2+' ve 56 tanesi 'Skor 3' olarak tanı konulmuş vakalardan elde edilmiştir. Hazırlanan bu veri kümesinin 105 tanesi eğitim kümesi, 86 tanesi ise test kümesi olarak ayarlanmıştır. Bu veri kümesinde invaziv tümör bölgesinde bulunan toplamda 62431 adet hücre saptanmış olup bu hücrelerin 24656 adedi eğitim için sınıflandırıcılara verilmiş olup geriye kalan kısmı test için kullanılmıştır. İkinci veri seti, Warwick Üniversitesi tarafından halka açık olarak erişilebilen bir veri kümesinden elde edilmiştir. Bu veri kümesinde 79 adet IHC ile boyanmış tüm slayt görüntüsü(Whole Slide Image-WSI) bulunmaktadır. Bunların 51 tanesi eğitim kümesi olarak, 28 tanesi test kümesi olarak ayarlanmıştır. Bu görüntüler çok büyük çözünürlükte oldukları için işlenmesi güçtür. Bu aşamada her bir görüntü 40X büyütmede, belirli boyutlarda(1376x1040) parçalara ayrılmış, içlerinden invaziv tümör bölgeleri tek tek seçilmiştir.

Elde edilen bu veri kümeleri öznitelik çıkarımı için uygun hale getirilir. Daha sonra, görüntüler hematoksilen (H) ve diaminobenzidin (DAB) renk kanallarına ayrılır ve hücre merkezleri ve hücre membranları belirlenir. Hücreler hematoksilen ile boyandıkları için mavi, tümör bölgeleri ise diaminobenzidin ile boyandıkları için kahverengi olarak görünür. Burada iki farklı boyayı birbirinden ayırıp tek bir kanal olarak elde edebilmek için Renk Dekonvolüsyonu(Color Deconvolution) yapılmaktadır. Renk Dekonvolüsyonu yönteminde her bir renk uzayı için belirlenmiş olan filtreler kullanılır. Örneğin bir IHC görüntüsü hematoksilen ve diaminobenzidin için oluşturulmuş filtreden geçirildiğinde sonuç olarak tek başına hematoksilen görüntüsü, tek başına diaminobenzidin görüntüsü ve arkaplan görüntüsü elde edilir. Hücre merkezlerinin belirlenmesinde hematoksilen görüntüsü bir takım eşikleme yöntemleri ile birlikte su yolu çizgisi(Watershed) yöntemi kullanılarak işlenir. Su yolu çizgisi yönteminde birbirine değen, üst üst gelmiş hücreler birbirlerinden ayrılmış olurlar ve hücre merkezleri doğru bir biçimde tespit edilir. Yine bir takım eşikleme yöntemleri(Otsu Thresholding) kullanılarak membran(tümör) bölgeleri diaminobenzidin görüntüsünden tespit edilir. Daha sonra, membran yoğunluğu histogramları(Membrane Instensity Histogram-MIH) olarak isimlendirilen görüntü analiz yöntemi ile bir takım öznitelik vektörleri çıkarılır, böylece her hücre için bir vektör elde edilir. Membran yoğunluğu histogramını elde ederken, daha önce bulunmuş olan hücre merkezlerinden yola çıkarak, hücre çeperinden 360 adet farklı piksel değeri elde edilir. Hücre merkezinden hücre çeperlerine doğru çekilen okların membran boyasına ilk ulaştığı yer ve sonrasındaki 10 noktanın piksel değerlerinin ortalaması alınır. Bu 360 noktanın 10 piksel kalınlıktaki çeperinden elde edilmiş ortalama piksel değerlerinin histogramı elde edilir ve bu histogram 16'ya kuantalanır. Burada belirtilen 10 piksel kalınlığı 2713 hücre örneğinden deneysel olarak test edilip elde edilen sonuçlara göre belirlenen membran kalınlığıdır. Bu, 40X büyütme kullanılarak elde edilen IHC ile boyanmış meme tümörü hücrelerinin ortalama membran kalınlığı 10 piksel olarak tanımlanır demektir. Sonuç olarak her bir hücre için 1x16'lık bir öznitelik vektörü elde edilmiş olur. Buradaki en büyük problem invaziv ve in situ tümörlerinin tespit edilmesidir. Kanserli doku üzerinde çoğu zaman invaziv bölgeleri ile in situ bölgeler birbirleri ile aynı özelliği göstermektedir. Ancak skorlama işlemi uygulanırken in situ bölgeler dikkate alınmamaktadır. Bu problemi aşmak için patologların görüşüne ihtiyaç duyulmaktadır. Patologların yardımı ile eğitim

kümesi oluşturulmuş ve bu küme tek tek işaretlenerek eğitim kümesi hazırlanmıştır. Elde edilen 1x16 boyutlu öznitelik vektörleri Z-Skorlama yöntemi kullanılarak normalize edilmiş ve sınıflandırıcılar için uygun hale getirilmiştir.

Son olarak, elde edilen özellikler Uzun-Kısa Süreli Bellek (LSTM), KNN, Karar Ağaçları gibi bazı sınıflandırıcılar ile eğitilerek, sınıflandırma modelleri oluşturulmuştur. Veri kümeleri hem hücre temelli hem de görüntü temelli olarak sınıflandırılmıştır. Hücre tabanlı sınıflandırmada her bir hücrenin skoru belirlenip gerçek skoru ile karşılaştırılır ve ona göre başarım çıkarılır. Görüntü tabanlı sınıflandırmada ise o görüntüde bulunan doku bölgesindeki bütün hücreler değerlendirilir ve yukarıda bahsedilen skorlama kurallarına göre(örn: Skor 3+ hücre sayısı %10'dan yüksek ise Skor 3.) sınıflandırma yapılır. LSTM sınıflandırıcısı kullanılırken maksimum devir sayısı(Maximum Epochs) 50 olarak belirlenmiş optimizasyon olarak da ADAM kullanılmıştır. Bunlara ek olarak bütün sınıflandırıcılarda 5 kat çapraz doğrulama(5 Fold Cross Validation) kullanılarak validasyon başarımları elde edilmiştir. 4 sınıf hücre temelli sınıflandırmadan oluşan CerbB2 puanlama sistemi,en yüksek başarımı Ensemble Boosted Trees yönteminde almış olup validasyon başarımlarında % 87,60 ve görüntü temelli test başarımlarında %91,43 doğrulukla benzer yöntemleri geride bırakmıştır. Hücreye dayalı sınıflandırma doğruluğu ise %77,56 ile karar ağacı sınıflandırıcıları kullanılarak elde edilmiştir ve gelecekteki çalışmalarda bu doğruluğun artırılabileceği öngörülmektedir. Bir tümör bölgesinde bütün hücre tiplerinden de bulunabilecek olması hücre tabanlı başarıma göre görüntü tabanlı başarımın düşük çıkmasına sebep olmaktadır. Çalışmadaki her adım ayrıntılı olarak açıklanmakta ve deneysel sonuçlar diğer son teknoloji yöntemlerle karşılaştırılarak sunulmaktadır.

1. INTRODUCTION

Today, breast cancer is one of the most well-known and the most under-researched cancer type in the world. Since technology has been developing day by day, detection of breast cancer and its treatment has been faster and accurate by co-working of various disciplines. In daily routine, cancer is diagnosed by pathologists, using light microscopes [3] in this way, the images seen on microscopy can also be used as an optical test sample. As a result, not only physicians are working on detection of cancer on tissue specimen, but also engineers could contribute to this process by technological developments. In this regard, both robotic devices and computer-assisted approaches have started to be used in the cancer diagnosis by microscopic image analysis [4]. Therefore, evaluation of tissue specimens became an engineering problem to be utilized by computer and electronical resources.

1.1 Purpose of Thesis

Although main aim of the microscopic image analysis which is a topic of digital pathology is to diagnose cancer, until now it is effectively used for cell counting, cell segmentation, and cell scoring [5]. There is interobserver discrepancy in most of the scoring systems used in pathology practice such as percentage of Ki67, ER, PR, Liver Steatosis [6]. In this point, computer-aided scoring systems could help to overcome this discrepancy problem, and speed up the process.

In the treatment of cancer, chemotherapy (CT) is a frequently used choice, but usual CT agents also damage native tissues as well as cancer cells [7]. Recent developments unabled physicians to use new methods termed 'targeted therapy' which only destroy the cancer cell, labeled by some cell markers [8]. CerbB2 is a transmembrane protein belonging to epidermal growth factor receptor (EGFR) family and located on the chromosome 17q12 is overexpressed in 15-20 % of the breast carcinomas [9] [10] [11]. CerbB2 mutated breast carcinomas have worse prognosis but are suitable for a targeted therapy agent called trastuzumab [12]. In CerbB2 mutated breast tumors, tumor cells

have increased CerbB2 protein, which is located on the cell membrane. Pathologists can detect CerbB2 overexpression with two methods. The gold standard method is In Situ Hybridization (ISH) that shows directly gene amplification on the chromosome [13]. Since this method is expensive, time consuming and not easily applicable, in practice, most laboratories use Immuno Histo Chemistry (IHC) at the first line [14]. By IHC, increased CerbB2 protein on the cell membrane is demonstrated by using antibodies against this protein, after protein-antibody binding, a stain, called chromogen, is used for visualization. With IHC, pathologist evaluates the intensity/darkness, continuity and the extensity of the stain in the tumor cells [15]. For standardization of the evaluation among pathologists and concordance with FISH (Fluorescent in Situ Hybridization) [16], ASCO/CAP 2013 score scale system recommendations are used [1]. According to these recommendations, tumors are categorized into four groups based on their staining observations, namely, Score 0+, Score 1+, Score 2+ and Score 3+ in Table 1.1 and Fig. 1.1. Tumors having Score 3+, are suitable for the treatment targeted CerbB2 protein. For tumors with Score 0+ and 1+, this therapy is not effective. Score 2+ is the borderline group which means some of the tumors with Score 2+ have CerbB2 mutations in DNA and can benefit from targeted therapy and some of them have not. Therefore, for this group of tumors, the gold standard method ISH must be used for higher accuracy [14] [15] [16] [1]. CerbB2 is a prognostic, predictive and therapeutic marker, but the targeted therapy against CerbB2 is expensive and have cardiotoxicity. Hence, it is important to choose correct patients. Also, there is an interobserver discrepancy among pathologists especially for tumors with Score 2, so determination of the tumor CerbB2 status is critical [17].

Table 1.1 : CerbB2 score scale system based on ASCO/CAP 2013 recommendations [1].

Score Type	***Definition***
Score 0 (negative)	No staining is observed or membrane staining that is incomplete and is faint/barely perceptible and within $\leq$10% of tumor cells.
Score 1 (negative)	Incomplete membrane staining that is faint/barely perceptible and within >10% of tumor cells.
Score 2 (equivocal)	Circumferential membrane staining that is incomplete and/or weak/moderate and within > 10% of tumor cells or complete and circumferential membrane staining that is intense and within $\leq$10% of tumor cells.
Score 3 (positive)	Circumferential membrane staining that is complete, intense, and within > 10% of tumor cells.

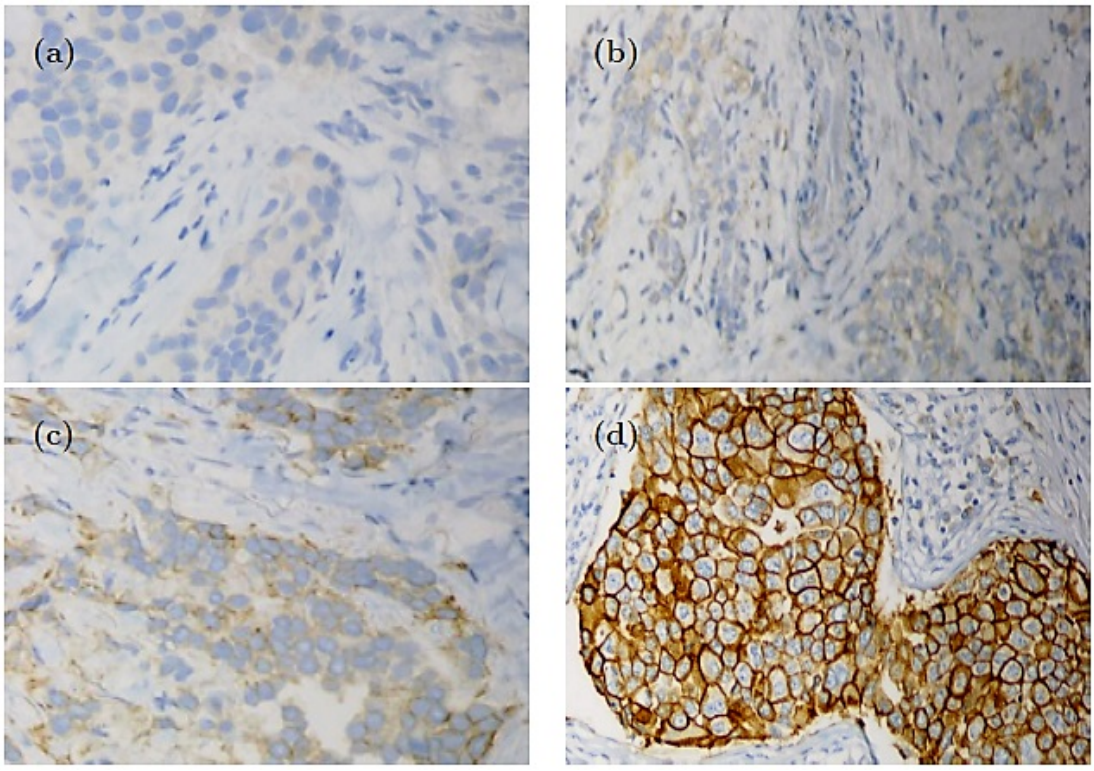

Figure 1.1 : Sample breast carcinoma tissue images with (a) Score 0+, (b) Score 1+, (c) Score 2+, and (d) Score 3+. Membranous staining becomes perceptible as scores increase. Tumors with a Score 3+ which have intense and uniform circumferential staining are considered as suitable for the targeted CerbB2 protein treatment by pathologists.

1.2 Literature Review

There are similar studies in the literature aiming at identifying CerbB2 mutated regions [18] [19]. The performance of the proposed method is compared with the free digital image analysis software presented in [18], which is the only available tool to realize automated tissue scoring [19]. A pixel-level feature set is extracted from HER2 stained tissue images to classify overexpressed and underexpressed regions. Different from the method in [19], a membrane based cell identification method is proposed to perform automated tissue scoring. Hence, tissue samples are classified in more than two classes. Cell detection stage of the proposed method is an extension of an earlier multi-level thresholding based study [20]. In addition to the multi-level thresholding based cell nucleus identification, cell membranes are also segmented by utilizing radial lines emanating from the center of the cell nucleus. In another study [21], the algorithm consists of three stages Color Pixel classification, cell nuclei segmentation and membrane staining classification. In first step, membrane pixels and cell nuclei pixels are taken out from image by using linear regression classifier. Then, Cell nuclei regions are obtained from the cell nucleus pixels extracted based on connected component analysis. At the last step, membrane completeness and staining intensity features are taken out by using cell nuclei regions. After that, these features are classified by using minimum cluster distance(MCD). Cordeiro et al. developed an algorithm [22]. In this algortihm, they used histogram inRGB and HSV color space in addition to mean and standard deviation per color channel in order to extrack color features. For texture features, they used different classifiers like lbp, pftas, svm, knn etc. In patient phase, they classified 250x250 size of patches by using SVM, MLP, KNN(k=1 best result) and decision tree classifiers. Ficarra et al. reported a method which consists of steps detection of cellular membrane, computation of approxiamate membrane, and detection of final cellular membrane [23]. In first phase, they described morphologh-based method to segment nuclear profiles [24] [25]. They used these nuclear profiles in order to detect cellular membranes. After that, voronoi diagrams [26] and delenuay triangulation [27] was used to find individual centers and approxiamate cellular membrane according to minimum distance criterion. Then, using a scanning procedure on approxiamate cell membrane with constant width, they extracted final cellular membrane. Di Cataldo

et al. have focused on unsupervised color clustering and automated segmentaiton of the cellular membrane based on color seperation and morphological processing [28] . In the first phase, color clustering is based on color deconvolution [2]. In second phase their method uses color and morphological information to extract cancerous tissue from non-cancerous region. In another method, Saha et al. proposed a productive deep learning model with minimum user effect. They called this model as Her2Net [29]. They developed a traezoidal LSTM connection topology to improve performance of proposed method. According to authors of the Her2Net, this procedure can be explained as a new way of segmentation of cell membrane and nucleus detection. In smilar approach [30] to the previous method, authors developed a convolution network. In cell segmentation phase, they used color deconvolution [2] method to extract each channel as H, DAB and background. Then, segmenting cells by using watershed algorithm from H channel. In cell classification phase, they used two different method like classical machine learning workflow with feature extraction and convolutional neural network(ConvNet). Chang et al. have extracted co-occurrence matrix features at feature extraction phase as Entropy, Angular Second Moment, Mean, Contrast, etc [31]. To eliminate these features the Sequential Floating Forward Selection(SFFS) [32] is used. In classification phase, authors benefited from three SVM classifiers to classify each cancer phases. In another method [33], authors used an active learning with deep network to detect cell membranes. The method was developed by using convolutional neural networks. This network was designed as a pixel classifier that classifies whether a pixel is membrane. In this [34] work, the authors used Convolution Network to classify CerbB2 whole slide images without neither membrane segmentation nor cell segmentation. They used 128x128 sized patches to classify images. They've had a success that can't be ignored. In various study in the literature, there are a lot of study for automated analysis and scoring of HER2(CerbB2) with high success results based on pixelwise analyse [35], color histogram [36], geometric features [37].

1.3 Hypothesis

In this study, in order to mitigate the interobserver discrepancy, novel image analysis methods are developed to determine the score of the CerbB2 tissue sample. For this purpose, tissue samples are analyzed on a cellular basis where each cell is identified using membrane based feature extraction and classification methods. This study was conducted by a group of computer scientists and medical researchers. Tissue specimens are prepared and sample images in Fig. 1.1 are acquired at the department of medical pathology, Medipol University Hospital, Istanbul and second datasets are acquired Computer Science Department, University of Warwick.
Contributions of this study are given as follows:

- a hybrid multi-level thresholding and radial line based cell detection method is developed,
- a Membrane Intensity Histogram (MIH) based cell identification method is developed,
- a tissue specimen image dataset is prepared,

for CerbB2 mutated breast carcinoma automated IHC stained tissue scoring purposes.

2. PROPOSED METHOD

Stages of the CerbB2 mutated breast carcinoma automated tissue scoring system are presented in Fig. 2.1 Sample tissue images, CerbB2 tissue specimen is divided into two sub-regions namely cell nuclei and cell membrane to benefit from pixel values of hematoxylin and diaminobenzidine which are used for background staining. Then multilevel thresholding is explained for detection of cell nuclei and cell membrane by using gray level binary images. In the last part, how the classes are grouped by using IHC, how the SVM classify the scores based on the features is explained in details of subsections in followings.

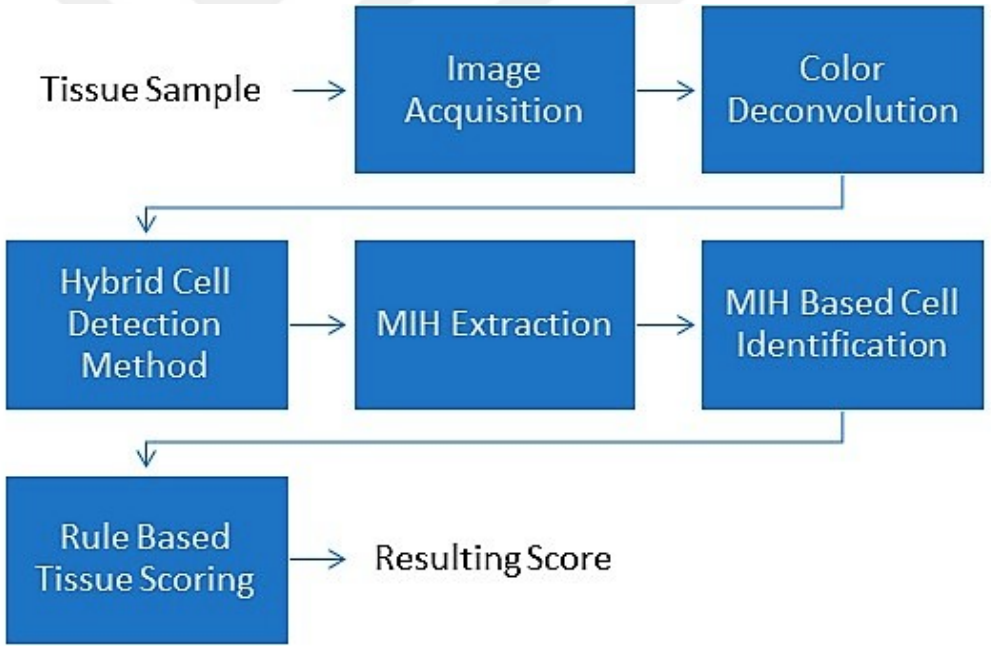

Figure 2.1 : Workflow of the proposed IHC Stained CerbB2 mutated breast carcinoma automated tissue scoring system. Tissue samples are fed into the system in order to obtain the resulting ASCO/CAP 2013 tissue score [1].

2.1 Color Deconvolution

Immuno Histo Chemistry (IHC) is a frequently used staining process for detection of antigens in tissue samples [38]. There are various histochemical staining methods developed for different proteins, cytoplasm, cell nuclei and cell membrane. The most common differential staining methods over the color approximations are hematoxylin (H-Blue) and diaminobenzidine (DAB-Brown) [2]. In this study, H and DAB colored digital pathology images are analyzed. Once the prepared tissue slides are digitized, acquired images are first decomposed into H and DAB color channels by the color deconvolution method in [2]. Color deconvolution method relies on the utilization of the so-called optical density matrix. Each stain type has its own optical density coefficients which are used to determine the corresponding transformation matrix, T. The transformation matrix for hematoxylin, eosin and DAB staining is shown in (Eq. 2.1).

$$T = \begin{bmatrix} 0.65 & 0.70 & 0.29 \\ 0.07 & 0.99 & 0.11 \\ 0.27 & 0.57 & 0.78 \end{bmatrix} \tag{2.1}$$

A sample result of the color deconvolution method is shown in Fig. 2.2, where the original digital pathology image is decomposed into DAB and Hematoxylin channels. These channels are used for ”hybrid cell detection” and ”Membrane Intensity Histogram (MIH)” based cell identification purposes. Let D be dab channel of the region of tissue, H be hematoxylin channel of the region of tissue.

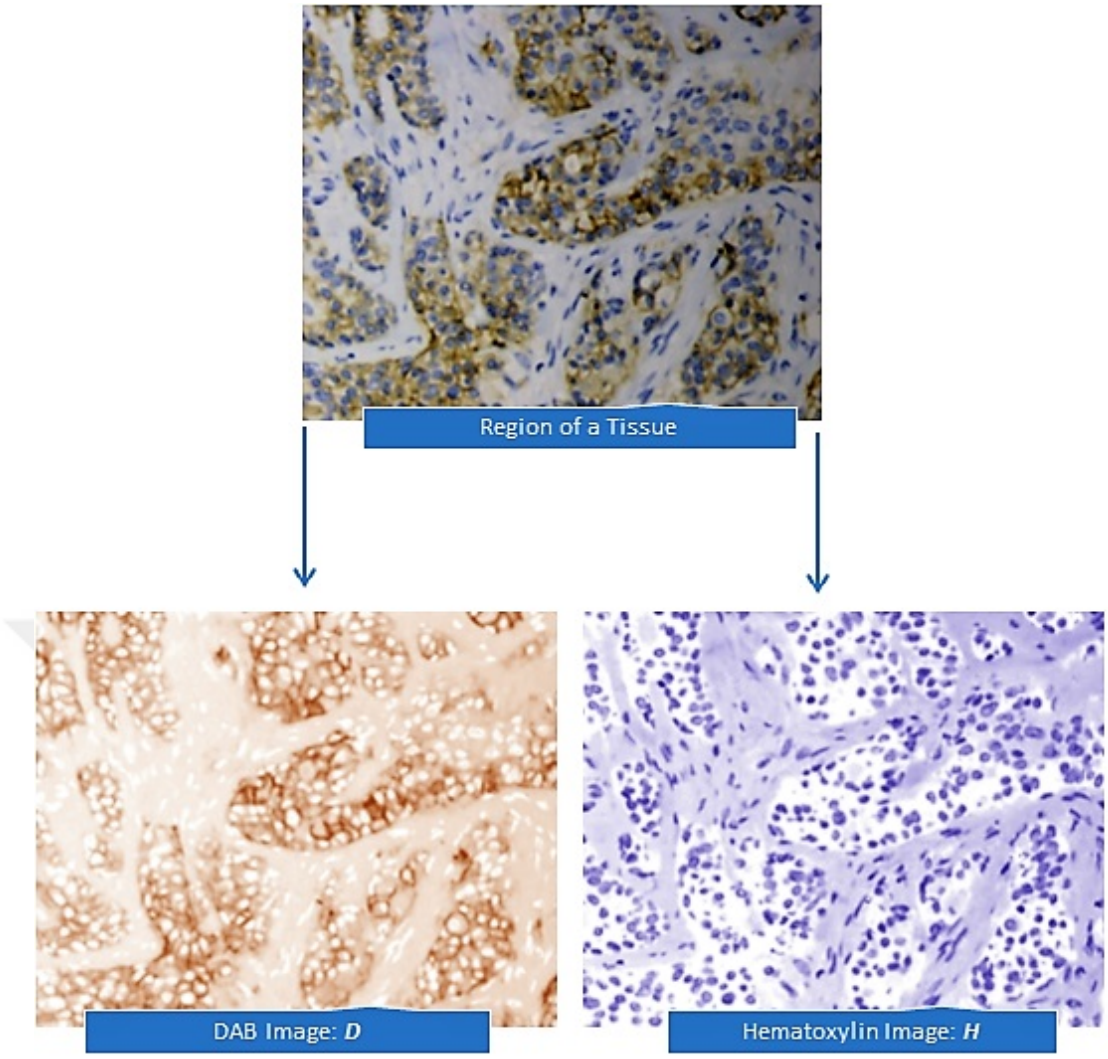

Figure 2.2 : Decomposition of H and DAB channels using the color deconvolution method in [2].

2.2 Hybrid Cell Detection Method

Once the image is decomposed into DAB (D-brown) and Hematoxylin (H-blue) channels, cell nuclei centers are determined by utilizing a multi-level thresholding based algorithm applied on Hematoxylin channel(H), and a radial line based cell membrane detection algorithms applied on DAB channel(D). These algorithms constitute the hybrid cell detection method.

2.3 Cell Nuclei Detection

Spatial high-frequency content within cell nuclei regions in Fig. 2.3(a) are suppressed by median filtering as in Fig. 2.3(b). This step is followed by Otsu thresholding method which finds the threshold that maximizes the between-class and minimizes the within-class variances of background and foreground regions [39]. The resulting binary image obtained by Otsu thresholding is shown in Fig. 2.3(c). The figure contains connected cell regions from which it is hard to determine separate nuclei centers. In order to mitigate this issue, a multi-level thresholding based approach is followed. This approach includes the distance transform stage in which regions with intensity values above the Otsu threshold are labelled with respect to their distance from the pixels with intensity values below the Otsu threshold in Fig. 2.3(d) [40]. This way, each cell nuclei center attains the local maximum distance label value. To determine local maxima, a multi-level thresholding approach is carried out by sweeping the whole dynamic range of intensity values from the highest to the lowest one. Masks obtained for a decreasing set of threshold values are shown in Figs.2.3(e)-2.3(h). Consequently, center pixels of cell nuclei, which happen to be the local-distance-label-value maxima, are determined, as shown in Fig. 2.3(i). The proposed cell nuclei detection algorithm is presented below. Let HB be binary image of H, HD be distance transform of HB :

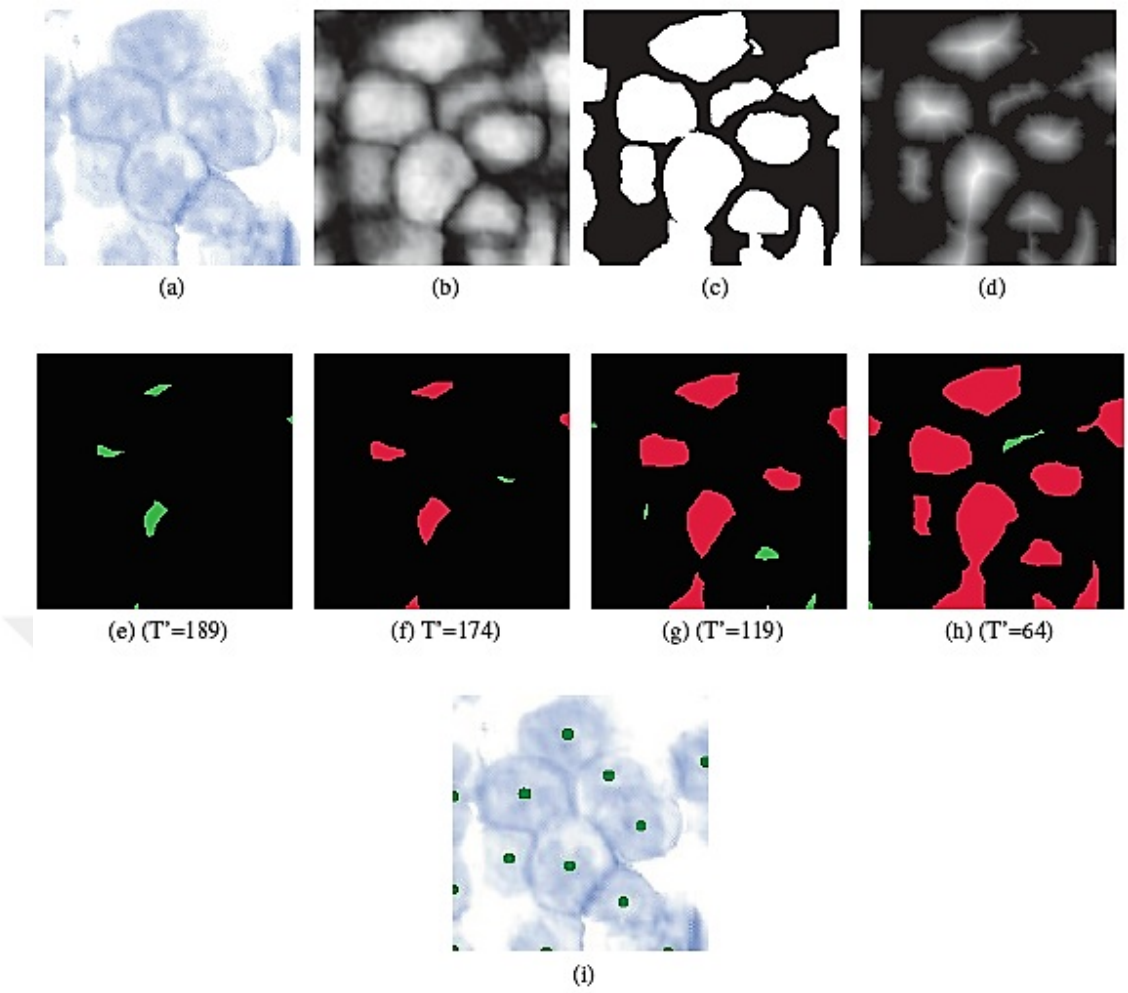

Figure 2.3 : Stages of the cell nuclei detection algorithm (a): Hematoxylin Image (H), (b): Gray Level Hematoxylin Image, (c): Binary Hematoxylin Image (HB) (d): Distance transformed mage (HD), (e-h): Images that are thresholded with different threshold value. Green parts of the cells that were detected for the first time by using different threshold value represent the first cell centers, and red parts of the cells represent cell centers that are already listed, (i): Result Image.

2.4 Cell Membrane Detection

Cell nuclei centers determined from the cell nuclei detection algorithm are fed as input to the cell membrane detection algorithm, as well as the binary mask obtained from the DAB channel after color deconvolution. Radial lines emanating from cell nuclei centers are traversed until the first DAB mask pixel is reached as shown in Fig. 2.4(a). The pixel location is kept in a list called ”membrane polygon points list”. This process is repeated for a full cycle around the cell nucleus to populate the membrane polygon

points list. Hence, the cell membranes around the cell nuclei are determined Fig. 2.4(b). Details of the algorithm are presented below in Algorithm 3.

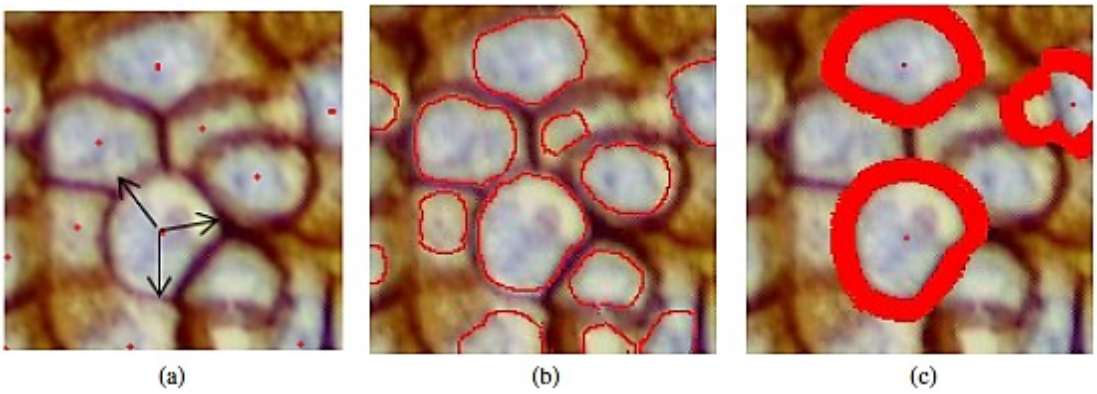

Figure 2.4 : (a) Radial lines (black arrows) emanating from cell nuclei centers (red dots) are traversed until the first DAB mask pixel is reached. (b) Cell membranes around the cell nuclei (red polygons) are determined by the "Cell Membrane Detection Algorithm". (c) Extended cell membrane region for MIH extraction.

Algorithm 1 Get Rounded Value Algorithm.

procedure GETROUNDEDVAL($valReal : Real$)
    $Result = Floor(valReal)$
    if $valReal \geq Result + 0.5$ **then**
        $Inc(Result)$
    end if
    Return *Result*
end procedure

Algorithm 2 Get Next Point Algorithm.

procedure GETNEXTPOINT($LineEq : Tline, Slope : Real$)
    if $(LineEq.m < 1)$ and $(LineEq.m \geq 0)$ **then**
        $Result.X := P_{cc}.X + ShiftVal$
        $Result.Y := GetRoundedVal(LineEq.GetYCoor(Result.X))$
    else if $(LineEq.m < 0)$ and $(LineEq.m > -1)$ **then**
        $Result.X := P_{cc}.X - ShiftVal$
        $Result.Y := GetRoundedVal(LineEq.GetYCoor(Result.X))$
    else
        $Result.Y := P_{cc}.Y + ShiftVal$
        $Result.X := GetRoundedVal(LineEq.GetXCoor(Result.Y))$
    end if
    Return *Result*
end procedure

Algorithm 3 Cell Membrane Detection Algorithm.

for $\Theta = 0 \rightarrow 359$ **do**
    $m := tan((\Theta * \Pi)/360)$;
    $LineEq := CreateLine(P_{cc}, m)$;
    for $i = 0 \rightarrow MaxShiftVal - 1$ **do**
        $NextP := GetNextPoint(LineEq, P_{cc}, i)$;
        if $R_{D_B}.PixelData[NextP.x, NextP.y] == 255$ **then**
            $PPList[m] := NextP$;
            $Break$
        else
            $Continue$;
        end if
    end for
end for

Let P_{cc} be cell center point, R_{D_B} be binary image of DAB channel of tissue region under consideration, Θ be angle of line, slope(m) be the slope of the straight line that comes from the center of the cell, createLine function creates line equation, MaxShiftVal is the farthest point to go, PPList is Cell Membrane Polygon point list.

It can be seen the visual expression of all stage of the Hybrid Cell Detection Method in Fig. 2.5.

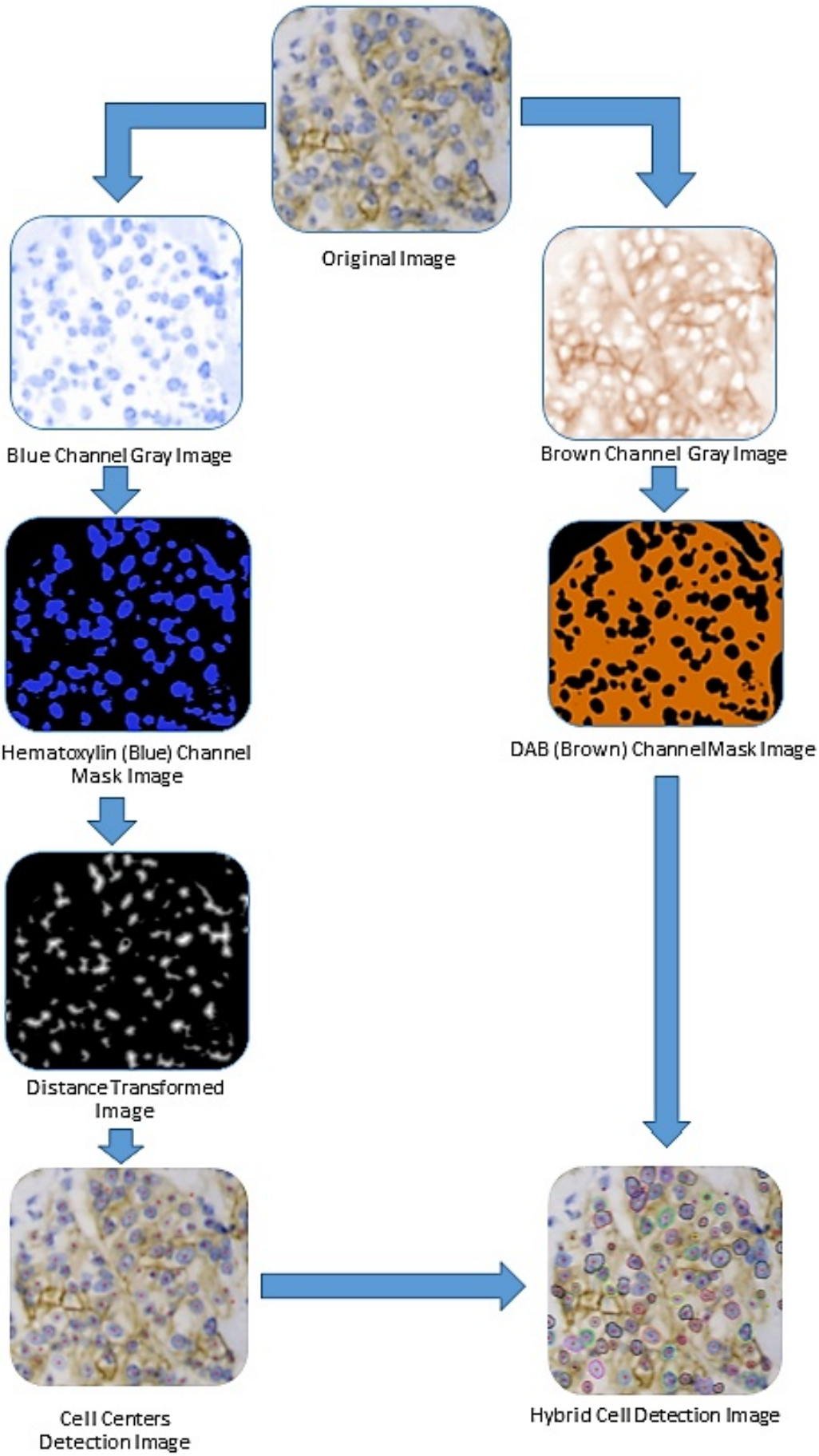

Figure 2.5 : Hybrid cell detection method.

2.5 Membrane Intensity Histogram (MIH) Extraction

Once the membrane polygon points lists are populated, neighboring pixels of membrane points extending outwards for a constant number of, d - many, pixels are further analyzed. To that extent, histograms corresponding to average intensity values of pixels around membrane points extending along each radial direction within a ring of width ”d pixels” encircling the membrane, are estimated. This d-many pixels are determined to be 10, which is the sum of the standard deviation and the average of the PDF obtained from the 2713 cells giving the figure 2.7. These histograms are called ”Membrane Intensity Histogram (MIH)” and they are used as feature vectors for cell identification. Average intensity values of 360 points in every cell which is occurred by cell membrane polygons. Then, 256 pixel values over the all points are quantized and 16 sized features are obtained in Fig. 2.9. At the fig. 2.8, average radius of the cells is 18,71. Accordingly, some of the 360 points will repeat themselves. This repeat does not change the characteristic properties of the membrane. In addition, since the radiuses of the cells are not very large, the algorithm will never skip information from the cell membrane. A sample histogram corresponding to the region is presented in Fig. 2.6.

For convenience, we adopt polar coordinates to represent pixel locations of the image I, as $I(r,\theta)$. Let O be the center point of the cell, $r(X)$ be the distance of a point X to O, and $\theta(X)$ be the angle between the positive-x axis and the ray $\overrightarrow{OX}$. Average intensity value of the membrane pixels along the $\theta - th$ direction, C_{Av_θ}, is defined as:

$$C_{Av_\theta} = \frac{1}{d} \sum_{r=r(A)}^{r(B)} I(r,\theta(A)) \tag{2.2}$$

Note that, $d = r(B) - r(A)$, and $\theta(A) = \theta(B)$. A visual representation for calculation of the C_{Av_θ} value is illustrated in Fig. 2.6.

For each cell, one gets 360-many C_{Av_θ} values. We apply a 16-bin uniform quantization on the histogram of these values to estimate the MIH-based features (cf. Fig. 2.9).

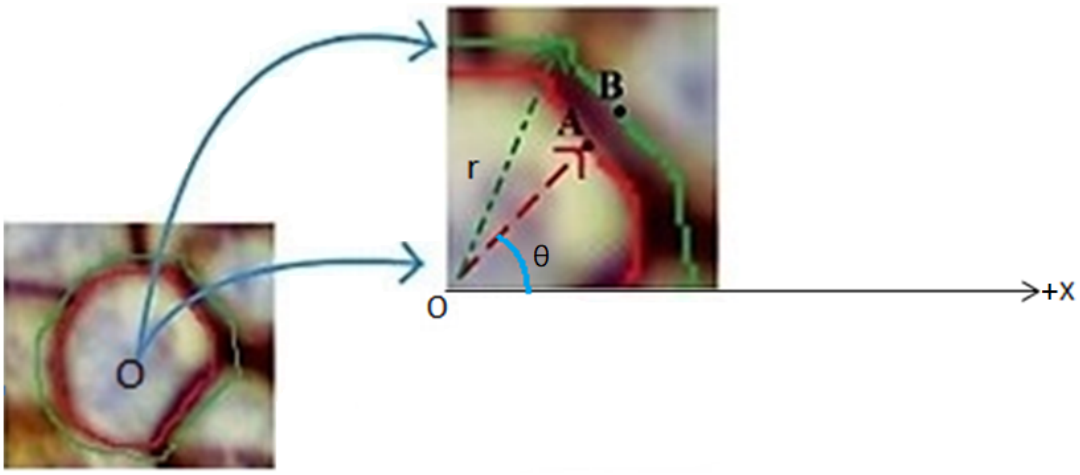

Figure 2.6 : Visual representation for calculation of the C_{Av_θ} value.

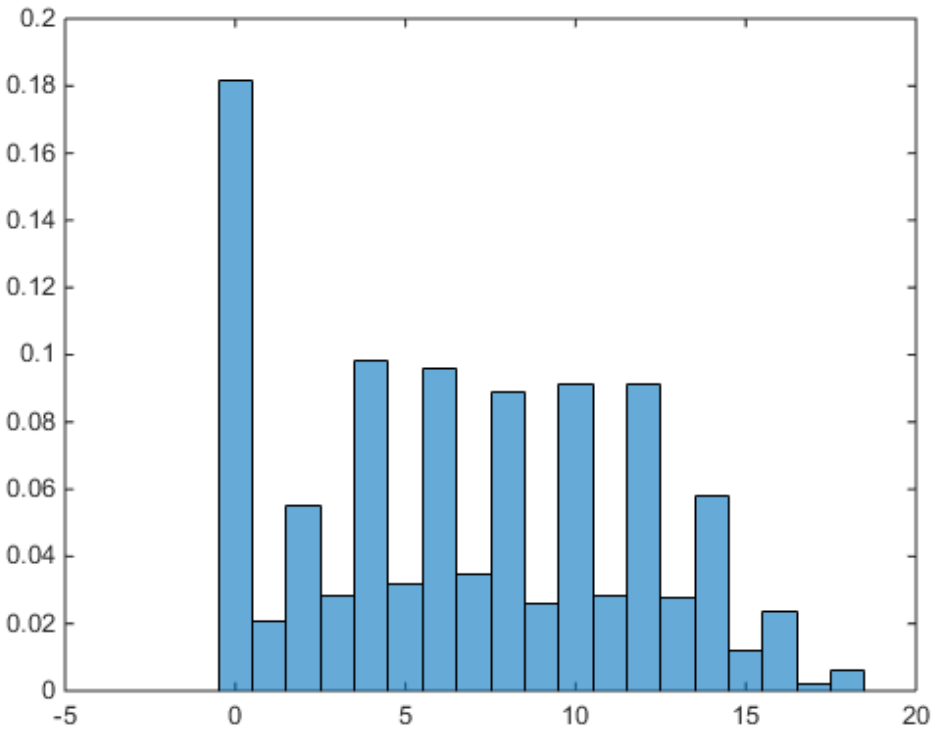

Figure 2.7 : Pdf of Membrane thickness of cells. Mean is 6.7 px, Standard Deviation is 4.86. This value and pdf is obtained from 2713 cells.

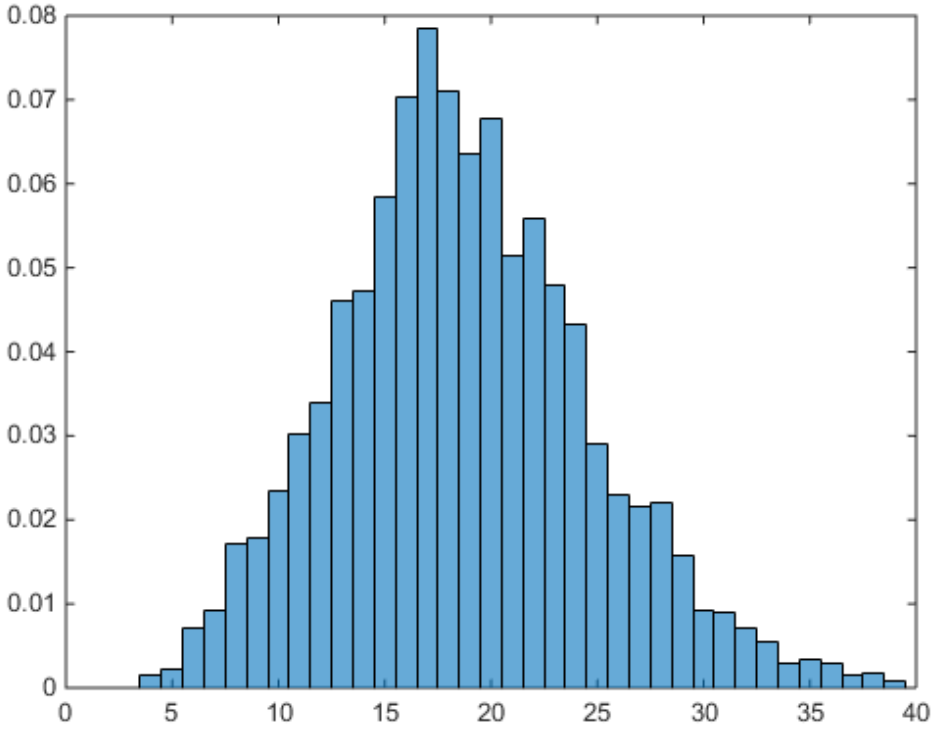

Figure 2.8 : Pdf of Radius of cells. Mean is 18.71 px, Standard Deviation is 5.95. This value and pdf is obtained from 2713 cells.

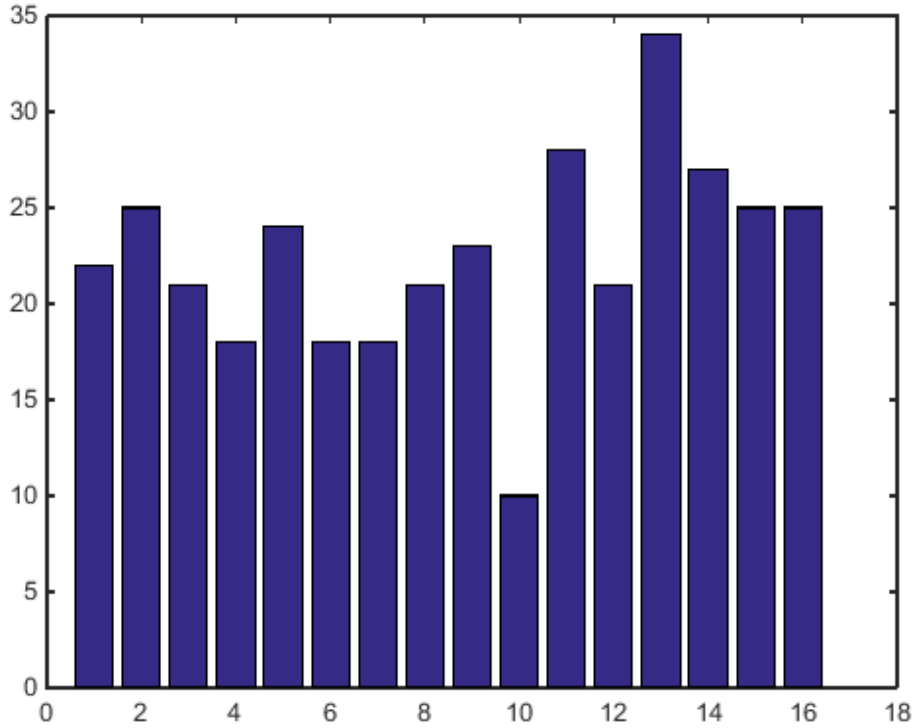

Figure 2.9 : Displaying of 16 sized vectors by quantizing 256 average pixel values of 360 points. Left: Number of Pixel, Bottom: Sixteen Level Histogram.

After creation of MIH vectors, labels (scores) are added for each image MIH vector as ”0”, ”1”, ”2”, ”3”. These labels were assigned knowledges that are shared by pathologists who have shared tissue specimen images, since the pathologists could analyze CerbB2 status of the tumor. These known labels are kept into an array lists corresponding to the related cells. In guidance of this studies, every label group is mapped to their correspondences for getting largest size of train labels, so it is obtained four main classes and this is followed by classification.

2.6 Membrane Intensity Histogram (MIH) Based Cell Identification

Membrane Intensity Histograms (MIHs) are used as feature vectors of size Q. These vectors are fed into a cell identification module utilizing LSTM and Classification Learner of MATLAB to classify MIH based features into four separate score classes, namely, Score 0+, Score 1+, Score 2+ and Score 3+ [41]. For identification purposes at the cellular level, a deep learning LSTM layers and a lot of decision trees classification method were used. Details of the training phase of classifiers are presented below.

These datasets are normalized by using Z-Score method which limits the value of train and test data between [-1,1] as advised in the method [42]. The normalized data set for the models planned to be created using different classifiers is appropriately separated for the training and testing phase. Then the 5 fold cross-validation method has been used to more accurately divide the test and training set [43]. Since 10 folds cross validation uses 90% of the data for the training, cross validation can cause wrong prediction of test performance. In this regard, 5 folds cross validation was prefered for training to improve robustness of the classifiers [44] [45] [46]. In figure 2.10, Hybrid Cell Detection Method and Membrane Intensity Histogram Extraction are presented by explaining step by step.

R_i: i^{th} Region of tissues.

R_{i_H}: Hematoxylin Channel of the i^{th} Region of Tissue.

C_i: i^{th} Cell of the i^{th} Region of Tissue.

R_{i_D}: DAB Channel of the i^{th} Region of Tissue.

C_{i_H}: Hematoxylin Channel of the i^{th} Cell.

C_{i_D}: DAB Channel of the i^{th} Cell.

$C_{i_{H_B}}$:Binary Image of Hematoxylin Channel of the i^{th} Cell.

$C_{i_{D_B}}$:Binary Image of DAB Channel of the i^{th} Cell.

H_i: Histogram of the i^{th} Cell.

$R_iC_jV_n$: n^{th} vector member of MIH vector of j^{th} cell of i^{th} Region of the tissue.

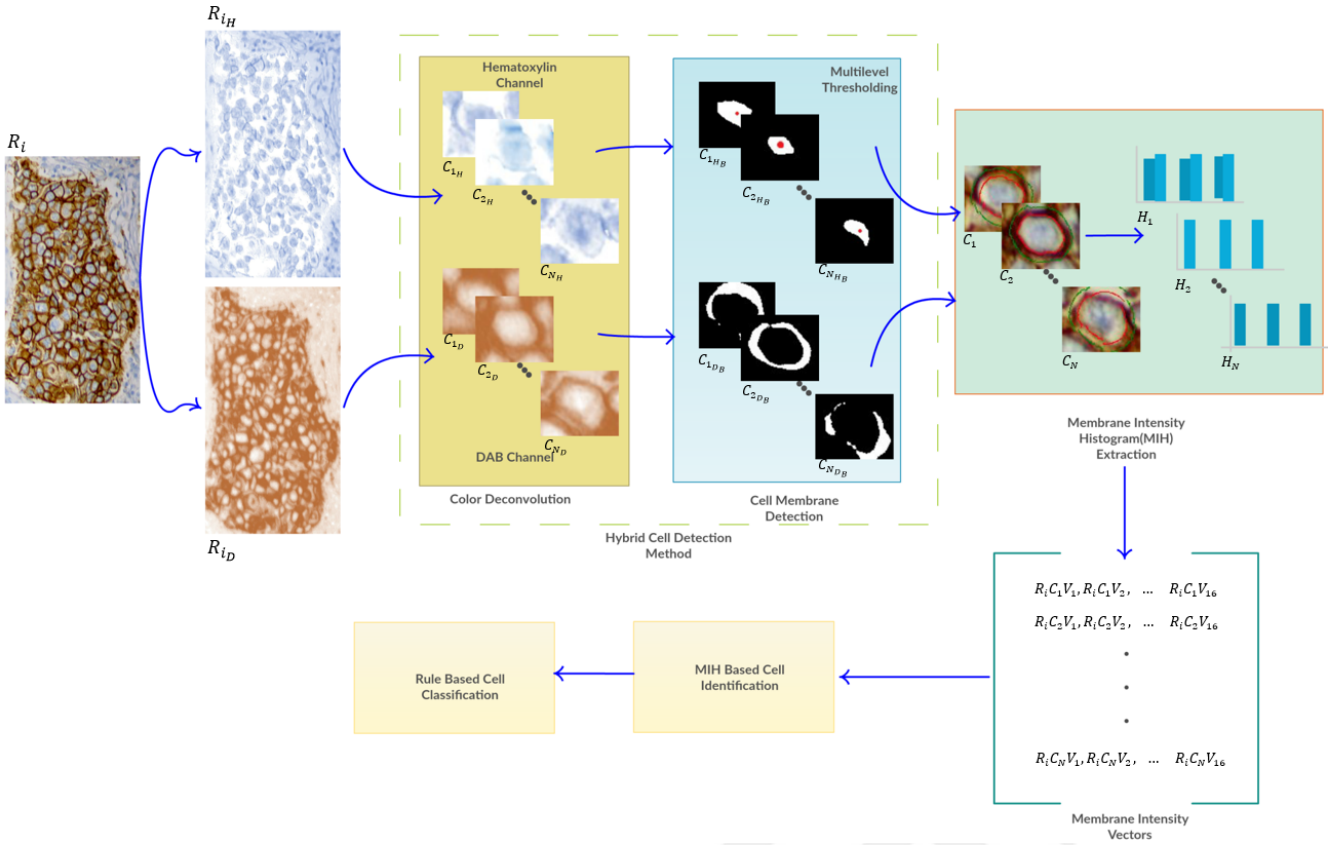

Figure 2.10 : Hybrid Cell Detection Method and Membrane Intensity Histogram Extraction.

20

2.7 Computational Complexity

According to all of the steps of the proposed method, let 'N' be the total number of pixels in a sample tissue image and 'm' be the number of cells in the image. Then, the complexity of the proposed method is given by:

$$O(N) + O(m) \tag{2.3}$$

Computational complexity can be seen in table 2.1 for per step.

Table 2.1 : Computational complexity per step.

Method	**Complexity**
Color Deconvolution	O(N)
Cell Detection	O(N)
MIH	O(m)
Identification	O(m)

3. EXPERIMENTAL SETUP

3.1 Data Set

In order to evaluate the scoring performance of the proposed technique, following experiments are carried out using two different databases. One of them is tissue specimens from patients with breast cancer at department of medical pathology, Istanbul Medipol University Hospital. Second one is the Department of Computer Science, University of Warwick, United Kingdom [47]. These specimens were processed over the tissue images consisting of cell patches are obtained to be analyzed for Computer Aided Diagnosis [48] [49].

First database are digitized by Argenit Kameram digital microscopy system, which consists of Zeiss Axio Scope A1 bright field microscope, 40X objective, 0.63X camera adaptor, Kameram 2 CCD camera (with 1.4 mega pixel sensor resolution), PC and Kameram software. The mosaic image acquisition tool of Kameram software is used to capture the panoramic images of tissue regions which are larger than the camera view area. Acquired images are further analyzed using a sequence of image analysis techniques developed specifically for automated tissue scoring. Second database were digitized by using Hamamatsu NanoZoomer C9600 scanner. The first database consists of 13 different cases and a total of 191 tissue images with 1360x1024(widthxheigth) resolutions, 105 of them were used for training, 86 of them were used for testing. 41 of them are diagnosed as 'Score 0+' (negative), 47 of them are diagnosed as 'Score 1+', 52 of them are diagnosed as 'Score 2+' and 56 of them are diagnosed as 'Score 3+' and, the dataset has number of 62431 cells.

These tissue images are arranged into files which consist of 4 main score classes and are shared accordingly in [50]. Also to the best of authors' knowledge, this is the second publicly available IHC stained tissue image data set for CerbB2 mutated breast carcinoma automated tissue scoring purposes after Warwick University [47]. The second database consists of 79 IHC stained Whole Slide Image(WSI) i.e 51 WSI for training and 28 WSIs for testing. These WSIs have size of 100000x80000(widthxheigth).

3.2 Patch Selection

In this step, feature extraction was applied without any changes in the resolution of the first database. In second database, WSIs were cropped at 40X magnification with size of 1376x1040(widthxheight) without any intersection between cropped images and without low resolution from mentioned resolution. After that, feature extraction was applied to the second database also. The biggest problem here is the detection of invasive and in situ tumors. In situ regions with invasive regions on cancerous tissue often show the same property with each other. However, in situ regions are not taken into account when scoring. In order to overcome this problem, the opinion of pathologists is needed. At this stage, in situ regions were extracted from the images obtained with the help of pathologists, and classifiers were given only cell features obtained from invasive regions.

4. EXPERIMENTAL RESULTS

These specimens that were mentioned in part 3.2 were processed over the tissue images consisting of cell patches are obtained to be analyzed for Computer Aided Diagnosis [48] [49]. All these tissue samples are diagnosed with cancer and scored by pathologists based on their own expertise and FISH technique which is accepted as the gold standard for breast cancer scoring [1]. Both database are trained by using Long-Short Term Memory(LSTM) layer and Classification Learner Tool of MATLAB. Classification learner tool of MATLAB was used to evaluate the scoring performance of proposed technique, several classifiers was used like Coarse Tree, Fine Tree, Ensemble-Bagged Tree, Fine KNN, Cosine KNN, Medium KNN etc. After the features were extracted by membrane intensity histogram using noval methods such as color deconvolution, multilevel thresholding and radial lines, first database was formed with 62431 cells from 198 tissue images. In first dataset 24656 cells, in second dataset 342568 cells that each cell is describing with 16 sized MIH vector were trained by using classification learner tool of MATLAB with 5 fold cross validation. In deep learning LSTM classifier, options were set as number of hidden units are 100, maximum epochs is 50, mini batch size is 27, adam [51] were used for optimization.

Accuracy which is shown as (Eq. 1.1), measures success of classifiers with proportion of number of correct prediction to total number prediction, is calculated as follows:

$$A = \frac{\sum_{l=0}^{n} P_l}{\sum_{l=0}^{n} T_l} x100 \tag{4.1}$$

where l express labels, P symbolize true predictions and T is used to represent total number prediction regardless of correctness.

In table 4.1, Warwick University datasets' tissue based Training Accuracy and their scoring systems Criteria 1 points that is mentioned in [47] can be seen. According to test results, Cosine KNN classifier gives highest result. Then, this point is ranked as 6th among the Her2Contest' contestants without bonus points and 7th with bonus

points. Satisfactory results were obtained from several classifiers, and the results that we obtained when we compared our scores with the scores of other competitors show the success of MIH method. People who share the second database with us only give us the ground truth of the training set. Since we don't have the ground truth of the test set, we're unable to report both cell-based and case-based test success. We sent them the scores we obtained as a result of the test and we can evaluate our position according to the other competitors by using the points sent to us according to their own scoring systems.

Table 4.1 : Performance of the classifiers on Warwick dataset.

CLASSIFIER	**Validation Accuracy**	**Her2Contest Points**	**Bonus Points**	**Total**
LSTM	%99.84	347,5	9,5	357
Disabled PCA	%99.99	355	2,5	357,5
Fine Tree	%99.99	367,5	6	373,5
Medium Tree	%99.99	332,5	14	346,5
Coarse Tree	%97.7	320	7	327
Fine KNN	%95.7	337,5	13,5	351
Medium KNN	%94.7	347,5	14	361,5
Coarse KNN	%91.1	347,5	**16**	363,5
Cosine KNN	%93.9	**385**	15	**400**
Weighted KNN	%95.4	322,5	12,5	335
Ensemble Bagged Trees	%99.9	322,5	12,5	335
Ensemble RUSBoosted	%99.3	322,5	12,5	335

Table 4.2 : Accuracy performances of MIH-based method with various classifiers on the clinical test dataset are presented in comparison with the ImmunoMembrane method in [17]. Samples presented in the test dataset consists of unseen data. Results indicate that MIH-based cell identification approach has higher accuracy independent of the classifier type. Best performing classifier and corresponding accuracy values are printed in boldface letters.

CLASSIFIER	**Validation Accuracy**	**Cell Based Scoring Accuracy**	**Tissue Based Scoring Accuracy**
LSTM	%88,01	%75,76	%89,52
Disabled PCA	%87,00	%75,99	%89,52
Fine Tree	%87,00	%75,99	%89,52
Medium Tree	%86,80	%76,26	%89,52
Coarse Tree	%85,60	%76,99	%84,76
Fine kNN	%82,60	%72,80	%83,80
Medium kNN	%86,40	%74,17	%89,52
Coarse kNN	%85,90	%73,68	%86,66
Cosine kNN	%85,70	%76,01	%88,57
Weighted kNN	%86,10	%74,17	%86,66
Ensemble Bagged Trees	%87,90	%77,39	%90,47
Ensemble Boosted Trees	**%87,60**	**%77,40**	**%91,43**
ImmunoMembrane [17]	-	-	%74,07

Table 4.2 shows cell based and tissue based performance of the proposed method on our clinical dataset. Validation accuracies as well as cell based and tissue based accuracies are reported for each classifier. As shown in the results, boosted tree based classifiers over-perform other classifiers both for cell based and tissue based tests.

4.1 Discussion

In recent years, the data used in many image analysis studies conducted with breast cancer data show a significant difference in terms of evaluation. These studies also differ in the use of different chemical dyes in the imaging of tissue samples taken from patients suspected of breast cancer. In this context, different from the type of chemical paint used in other works, IHC biomarker was used for the screening of tissue samples in this study. Then the results of image analysis were compared with the studies using the same chemistry to screen tissue specimens. These comparisons were executed based on the Warwick datasets [47] and higher performance achievements were got then some competitors. Compared to Vandenberghe et al.(2017) [30] results of first dataset, the 78% performance achieved by patch based classification and CNN use is lower than our 91,43% patch based performance.

In table 4.3 and table 4.4, bold cells represent accurate prediction of every scores as score 0+, score 1+, score 2+, score 3+ respectively. Intersection of columns and rows show accurate predictions in terms of cell number. Column which is called “Actual” shows cell based total test numbers in each Scores. “Recall” and “Precision” shows cell based accuracy for each type of score. While “Precision” shows predicted accuracy rate, “Recall” presents actual accuray rate. As it is expected, overall test accuracies are between precision and recall with 76,72% for Cell Based Tissue Scoring, 91,79% for Patch Based Tissue Scoring. This confusion matrices shows results of Cosine KNN classifier which gives best result for patch based classification. The confusion matrices in table 4.4 provides test accuracy with each type of score, it also represents data distribution. Since Score 2+ has the most confusion between score types, the least accuracy is obtained in Score 2+ for cell based tissue scoring. In patch phase Score 0+&1+ has most confusion, and the least accuracy obtained in Score 0+&1+. On the other hand, wrong prediction in test has caused lower accuracy rate, even though the related score type has high accuracy rates in actually. The most important cause of the error is the cytoplasmic staining. In cases where membrane staining was not present but in which cytoplasmic staining was occurring, it was seen that 0+ and 1+ cases behaved as 2+.

Table 4.3 : Demonstration of confusion matrices of cell based test data.

SCORES	**0 & 1+**	**2+**	**3+**	**Actual**	**Recall**
0 & 1+	**9962**	1423	60	11445	87,04%
2+	1794	**3967**	124	5885	67,40%
3+	1365	1015	**5868**	8248	71,14%
Predicted	13121	6405	6052	**25578**	75,19%
Precison	75,92%	61,93%	96,95%	78,26%	**76,72%**

Table 4.4 : Demonstration of confusion matrices of patch based test data.

SCORES	0 & 1+	2+	3+	Actual	Recall
0 & 1+	35	10	0	45	77,77%
2+	0	27	0	27	100%
3+	0	0	33	33	100%
Predicted	35	37	33	105	92,59%
Precison	100%	72,97%	100%	90,99%	91,79%

5. CONCLUSION

A novel image analysis based automated tissue scoring system is developed to determine the score of CerbB2 receptors in breast cancer tissue specimen images of patients with suspected breast cancer. The contributions of the study are summarized as:

- The development of a hybrid multi-level thresholding and radial line based cell detection method,
- The development of a Membrane Intensity Histogram (MIH) based cell identification method, and,
- The preparation of a tissue specimen image dataset for automated scoring of CerbB2 Receptors.

This study differs substantially from state-of-the-art computer-aided detection methods, such as the ones using Convolutional Neural Networks [52], as the proposed automated scoring system depends on dedicated methods exploiting various aspects of breast cancer tissue specimen images. The currently used first data set in this study are already available online [50] and this contribute the work specificity. The histogram obtained at the MIH stage of the proposed method is a unique method for understanding both completeness and membrane staining of tissue. The 360 different point values are useful for understanding the completeness in terms of circular information, and the pixel value of each point indicates the extent of membrane staining. To classify by using raw image and CNN classifiers seems to be advantageous in terms of achieving higher performance more quickly considering today's CPU and GPU capacities. However, it is more cost-effective to produce problem-specific solutions by feature extraction which is one of the basic principles of image processing. It also makes great contributions to academic knowledge. The proposed system is anticipated to assist pathologists by not only providing an image analysis based scoring tool, but also by mitigating the interobserver discrepancy.In some cases, pathologists may not be able to decide on their own. In such cases, two options emerge. The first is to consult with a specialist or group

of experts they think is better than their own. The second is to diagnose FISH, which is a much more expensive method. The second method is often not preferred because of its cost. Therefore, our goal is to develop a system that can offer additional consultation to pathologists.

REFERENCES

[1] **Wolff, A. C., H.M.E.H.H.D.G.D.M..H.W.** (2013). Recommendations for human epidermal growth factor receptor 2 testing in breast cancer: American Society of Clinical Oncology/College of American Pathologists clinical practice guideline update, *Journal of clinical oncology 31.31 : 3997-4013*.

[2] **Ruifrok, A.C. and Johnston, D.A.** (2001). Quantification of histochemical staining by color deconvolution, *Analytical and quantitative cytology and histology 23.4 : 291-299*.

[3] **Hecke, D.V.** (2002). Routine immunohistochemical staining today: choices to make, challenges to take, *Journal of histotechnology 25.1: 45-54*.

[4] **Esgiar, A. N., N.R.N.S.B.S.B.M.K..M.A.**, (1998). Microscopic image analysis for quantitative measurement and feature identification of normal and cancerous colonic mucosa, IEEE, 2.3 edition.

[5] **Wang, Y., Q.Y.T.T.M.K..Z.B.** (2017). A two-step convolutional neural network based computer-aided detection scheme for automatically segmenting adipose tissue volume depicting on CT images, *Computer Methods and Programs in Biomedicine 144: 97-104*.

[6] **Loukas, C.G. and Linney., A.**, (2004). A survey on histological image analysis-based assessment of three major biological factors influencing radiotherapy: proliferation, hypoxia and vasculature.

[7] **Wu, William W., M.G. and Lu., D.** (2014). Cytopathologic, histopathologic, and immunohistochemical features of intrahepatic clear cell bile duct adenoma: a case report and review of the literature, *Case reports in pathology 2014*.

[8] **Sawyers, C.** (2004). Targeted cancer therapy, *Nature 432.7015 : 294-297*.

[9] **Johnson, Kirby L., D.K.Z. and Bianchi., D.W.** (2000). The use of fluorescence in situ hybridization (FISH) on paraffin-embedded tissue sections for the study of microchimerism, *Biotechniques 29.6 : 1220-1224*.

[10] **Atkins, D., R.K.A.T.C.L.W.H..S.S.** (2004). Immunohistochemical detection of EGFR in paraffin-embedded tumor tissues: variation in staining intensity due to choice of fixative and storage time of tissue sections, *Journal of Histochemistry & Cytochemistry 52.7 : 893-901*.

[11] **Garrison, L.P. and Veenstra., D.L.** (2009). The economic value of innovative treatments over the product life cycle: the case of targeted trastuzumab therapy for breast cancer, *Value in health 12.8 : 1118-1123*.

[12] **N., Flanagan, L.H.J.G.J.M..Q.C.M.** (2016). New ASCO/CAP guideline recommendations for HER2 testing increase the proportion of reflex in situ hybridization tests and of HER2 positive breast cancers, *Virchows Archiv 468.2 : 207-211*.

[13] **Mass, R. D., P.M.F.A.S.C.M.A..S.D.J.** (2005). Evaluation of clinical outcomes according to HER2 detection by fluorescence in situ hybridization in women with metastatic breast cancer treated with trastuzumab, *Clinical breast cancer 6.3 : 240-246*.

[14] **Hammond, M.E.H. and Hicks, D.G.** (2015). American Society of Clinical Oncology/College of American Pathologists human epidermal growth factor receptor 2 testing clinical practice guideline upcoming modifications: proof that clinical practice guidelines are living documents, *Archives of pathology & laboratory medicine 139.8 : 970-971*.

[15] **Di Cataldo, S., F.E.A.A..M.E.** (2010). Automated segmentation of tissue images for computerized IHC analysis, *Computer methods and programs in biomedicine 100.1 : 1-15*.

[16] **Rakha, E. A., S.J.L.A.H..E.I.O.** (2014). The updated ASCO/CAP guideline recommendations for HER2 testing in the management of invasive breast cancer: a critical review of their implications for routine practice, *Histopathology 64.5 : 609-615*.

[17] **Layfield, L. J., F.S.E.M..S.R.L.** (2016). Interobserver reproducibility for HER2/neu immunohistochemistry: A comparison of reproducibility for the HercepTest^{TM} and the 4B5 antibody clone, *Pathology-Research and Practice 212.3 : 190-195*.

[18] **Helin, H. O., T.V.J.Y.O.H.H.J..I.J.** (2016). Free digital image analysis software helps to resolve equivocal scores in HER2 immunohistochemistry, *Virchows Archiv 468.2 : 191-198*.

[19] **Pezoa, R., M.F.C.A.P.H..T.C.** (2016). Segmentation of HER2 protein overexpression in immunohistochemically stained breast cancer images using Support Vector Machines, *Journal of Physics: Conference Series. Vol. 762. No. 1. IOP Publishing*.

[20] **Kabakci, K. A., C.A.T.B.U.A.M..A.L.D.** (2016). A multi-level thresholding based segmentation method for microscopic fluorescence in situ hybridization (FISH) images, *24th. Signal Processing and Communication Application Conference (SIU)*.

[21] **Masmoudi, H., H.S.M.P.N.M.K.J..G.M.A.** (2009). Automated quantitative assessment of HER-2/neu immunohistochemical expression in breast cancer, *IEEE transactions on medical imaging 28.6 : 916-925*.

[22] **Cordeiro, C. Q., I.S.O.A.J.H..O.L.F.** (2018). An Automatic Patch-based Approach for HER-2 Scoring in Immunohistochemical Breast Cancer Images Using Color Features, *arXiv preprint arXiv:1805.05392*.

[23] **Ficarra, E., D.C.S.A.A..M.E.** (2011). Automated segmentation of cells with IHC membrane staining, *IEEE Transactions on Biomedical Engineering 58.5 : 1421-1429*.

[24] **S. D. Cataldo, E.F. and Macii, E.** (2007). Selection of tumor areas and segmentation of nuclear membranes in tissue confocal images: A fully-automated approach, *IEEE International Conference on Bioinformatics and Biomedicine (BIBM 2007)*.

[25] **S. D. Cataldo, E. Ficarra, A.A. and Macii, E.** (2008). Segmentation of nuclei in cancer tissue images: Contrasting active contours with morphology-based approach, *8th IEEE International Conference on BioInformatics and BioEngineering*.

[26] **Aurenhammer, F. and Klein, R.**, (2000). Voronoi diagrams, Elsevier.

[27] **Fukuda, K.**, (2000), Frequently asked questions in polyhedral computation [Online], `Available:http://www.ifor.math.ethz.ch/fukuda/polyfaq/polyfaq.html`.

[28] **Di Cataldo, S., F.E.A.A..M.E.** (2010). Automated segmentation of tissue images for computerized IHC analysis, *Computer methods and programs in biomedicine 100.1 : 1-15*.

[29] **Saha, M. and Chakraborty, C.** (2018). Her2net: A deep framework for semantic segmentation and classification of cell membranes and nuclei in breast cancer evaluation, *IEEE Transactions on Image Processing 27.5 : 2189-2200*.

[30] **Vandenberghe, M. E., S.M.L.S.P.W.S.M..B.C.** (2017). Relevance of deep learning to facilitate the diagnosis of HER2 status in breast cancer, *Scientific reports 7 : 45938*.

[31] **Chang, Chuan-Yu, Y.C.H. and Ko., C.C.** (2012). Automatic analysis of HER-2/neu immunohistochemistry in breast cancer, *Innovations in Bio-Inspired Computing and Applications (IBICA), 2012 Third International Conference on. IEEE*.

[32] **Pudil, P., F.F.J.N.J..K.J.** (1994). Floating search methods for feature selection with nonmonotonic criterion functions, *Proceedings of the 12th IAPR International Conference on Pattern Recognition, Vol. 3-Conference C: Signal Processing (Cat. No. 94CH3440-5). Vol. 2. IEEE*.

[33] **Gaur, U., K.M.N.S.E.S.W..M.B.S.** (2016). Membrane segmentation via active learning with deep networks, *Image Processing (ICIP), 2016 IEEE International Conference on. IEEE*.

[34] **T. Pitkaaho, T. M. Lehtimaki, J.M. and Naughton, T.J.** (2016). Classifying HER2 breast cancer cell samples using deep learning, *Proc. Irish Mach. Vis. Image Process. Conf., pp. 1–104*.

[35] **Brügmann, A., E.M.L.G.N.S..V.M.** (2012). Digital image analysis of membrane connectivity is a robust measure of HER2 immunostains, *Breast cancer research and treatment 132.1 : 41-49*.

[36] **Keller, Brad, W.C. and Gavrielides, M.A.** (2012). Quantitative assessment and classification of tissue-based biomarker expression with color content analysis, *Archives of pathology & laboratory medicine 136.5 : 539-550*.

[37] **Laurinaviciene, A., D.D.O.V.J.S..L.A.** (2011). Membrane connectivity estimated by digital image analysis of HER2 immunohistochemistry is concordant with visual scoring and fluorescence in situ hybridization results: algorithm evaluation on breast cancer tissue microarrays, *Diagnostic pathology 6.1 : 87*.

[38] **Ramos-Vara, J.A. and Miller, M.A.** (2014). When tissue antigens and antibodies get along: revisiting the technical aspects of immunohistochemistry—the red, brown, and blue technique, *Veterinary pathology 51.1 : 42-87*.

[39] **Otsu, N.** (1979). A threshold selection method from gray-level histograms, *IEEE transactions on systems, man, and cybernetics 9.1 : 62-66*.

[40] **Danielsson, P.E.** (1980). Euclidean distance mapping, *Computer Graphics and image processing 14.3 : 227-248*.

[41] **Lo, C.S. and Wang, C.M.** (2012). Support vector machine for breast MR image classification, *Computers & Mathematics with Applications 64.5 : 1153-1162*.

[42] **Caruana, R. and Niculescu-Mizil, A.** (2006). An empirical comparison of supervised learning algorithms, *Proceedings of the 23rd international conference on Machine learning. ACM*.

[43] **Arlot, S. and Celisse, A.** (2010). A survey of cross-validation procedures for model selection, *Statistics surveys 4 : 40-79*.

[44] **An, Senjian, W.L. and Venkatesh, S.** (2007). Fast cross-validation algorithms for least squares support vector machine and kernel ridge regression, *Pattern Recognition 40.8 : 2154-2162*.

[45] **Dietterich, T.** (1995). Overfitting and undercomputing in machine learning, *ACM computing surveys (CSUR) 27.3 : 326-327*.

[46] **Reunanen, J.** (2003). Overfitting in making comparisons between variable selection methods, *Journal of Machine Learning Research 3.Mar : 1371-1382*.

[47] **Qaiser, T., M.A.R.P.C.M.S.D.T.V..M.R.** (2018). HER 2 challenge contest: a detailed assessment of automated HER 2 scoring algorithms in whole slide images of breast cancer tissues, *Histopathology, 72(2), 227-238*.

[48] **Doi, K.** (2007). Computer-aided diagnosis in medical imaging: historical review, current status and future potential, *Computerized medical imaging and graphics 31.4 : 198-211*.

[49] **Sajn, L. and Kukar., M.** (2011). Image processing and machine learning for fully automated probabilistic evaluation of medical images, *Computer methods and programs in biomedicine 104.3 : e75-e86*.

[50] **Kabakci, K.A., C.A.T.B.U..**, Regional Tissue Samples of Immunohistochemistry Stained Breast Cancer, `https://kovan.itu.edu.tr/index.php/s/Ey3dCu14SCK18of`.

[51] **Kingma, D.P. and Ba., J.L.** (2014). Adam : A method for stochastic optimization, *arXiv:1412.6980v9*.

[52] **Arevalo, J., G.F.A.R.P.R.O..L.M.A.G.** (2016). Representation learning for mammography mass lesion classification with convolutional neural networks, *Computer methods and programs in biomedicine 127 : 248-257*.

CURRICULUM VITAE

Name Surname : Kaan Aykut KABAKÇI

Place and Date of Birth: Kayseri-07.01.1993

E-Mail :kabakcik@itu.edu.tr & kaanaykutkabakci@gmail.com

EDUCATION:

- **B.Sc. :** 2016, Istanbul Technical University, Faculty of Electrical-Electronics, Electronics and Communication Engineering

PROFESSIONAL EXPERIENCE AND REWARDS:

- My graduation project named "Development of Cell Detection and Segmentation Methods in Fluorescent Pathological Images" was awarded the third prize in Arı Teknokent Graduation Design Projects competition.
- My graduation project named "Development of Cell Detection and Segmentation Methods in Fluorescent Pathological Images" was awarded with 2nd prize in TUBITAK Industry Focused Graduation Thesis Competition.

PUBLICATIONS, PRESENTATIONS AND PATENTS ON THE THESIS:

- **Kaan A. Kabakçı**, Abdulkerim Çapar, B. Uğur Töreyin, Mertkan Akkoç, Ozan Borazan, İlknur Türkmen, Lütfiye Durak Ata, A Multi-level Thresholding Based Segmentation Method for Microscopic Fluorescence In Situ Hybridization (FISH) Images, 978-1-5090-1679-2/16/$31.00 ©2016 IEEE, Sinyal İşleme ve İletişim Uygulamaları 2016
- Tataroğlu, G. A., Genç, A., **Kabakçı, K. A.**, Çapar, A., Töreyin, B. U., Ekenel, H. K., ... Çakır, A. (2017, May). A deep learning based approach for classification of CerbB2 tumor cells in breast cancer. In 2017 25th Signal Processing and Communications Applications Conference (SIU) (pp. 1-4). IEEE.